

SOURCE LOCALIZATION IN A WAVEGUIDE WITH UNKNOWN ACOUSTIC PROPERTIES

W A Kuperman & M D Collins

Naval Research Laboratory, Washington, DC, USA

1. INTRODUCTION

Conventional plane-wave beamforming has been generalized to source localization in a waveguide [1,2]. Matched-field processing (MFP) determines source location by comparing acoustic data with solutions of the wave equation for a large number of test source locations. This method breaks down if the acoustic properties of the waveguide are not known accurately, a situation referred to as mismatch [3]. In large regions of the ocean, environmental information is difficult to obtain due to oceanographic variations.

This paper describes a generalization of MFP that does not require accurate knowledge of the waveguide and hence bypasses the mismatch problem. Focalization combines source localization and a simultaneous search for the waveguide properties. The primary goal of focalization is to determine source location. Due to a parameter hierarchy in which source location outranks waveguide properties, focalization often determines the correct source location without determining the correct waveguide properties. With sufficient acoustic data, it is possible to determine the waveguide properties with focalization.

We have implemented focalization using simulated annealing [4,5] to search for the source location and environment that minimizes a cost function. This Monte Carlo optimization method involves randomly selecting perturbations of the search parameters and deciding whether or not to accept the perturbed parameters based on the change in the cost function, a Boltzmann probability distribution, an artificial control parameter that is analogous to temperature, and a sequence of random numbers.

2. RAY-BASED FOCALIZATION

In this section, we describe a focalization method based on a ray representation of the acoustic field. For a high-frequency source near the ocean surface, the nearfield resembles the Lloyd's mirror beams due to a point source in an infinite half space [6]. At long ranges, the Lloyd's mirror beams are bent by refraction and repeatedly reflect from the ocean surface (or turn over) at the convergence zones.

A qualitative representation of the acoustic field is obtained by tracing rays in the directions corresponding to the Lloyd's mirror beams from the point on the ocean surface directly above the source. The beams incident on a vertical array of hydrophones are represented by rays that originate at the centers of the beams and propagate in the directions of the beams. If the sound-speed distribution is known, the rays are traced away from the array and the rays focus near the ocean surface at the source range. The source depth can be determined by the Lloyd's mirror beam pattern.

If the sound-speed distribution is not known, it is adjusted using a search algorithm until the rays focus at a point near the ocean surface. The rays are traced for each test sound-speed distribution. The cost function E is defined as

SOURCE LOCALIZATION

$$E = \min_r F(r), \quad (1)$$

$$F(r) = \sqrt{\frac{1}{N} \sum_{n=1}^N z_n(r)^2}, \quad (2)$$

where the ray $z_n(r)$ corresponds to the n th beam and N is the number of beams. Focalization involves searching for the minimum of E . At each iteration, the estimate of the source range is the range at which F is minimized.

We illustrate ray-based focalization with Example 1, which involves a source at $r = 400$ km and the Munk sound-speed profile [7]. The Munk profile has a minimum value at the channel depth $z = z_0$, which is taken to be a piecewise-linear function of range. The back-propagated rays appear in Figure 1 at various stages of the search. The rays are initially far out of focus. At 40 iterations, the rays are attempting to focus at $r = 450$ km. The algorithm locks in to the correct source range after 100 iterations, and the rays are sharply focused at the ocean surface at the source range after 200 iterations. The energy, range estimates, and channel depth estimates appear in Figure 2. The range and channel depth estimates converge to the correct values.

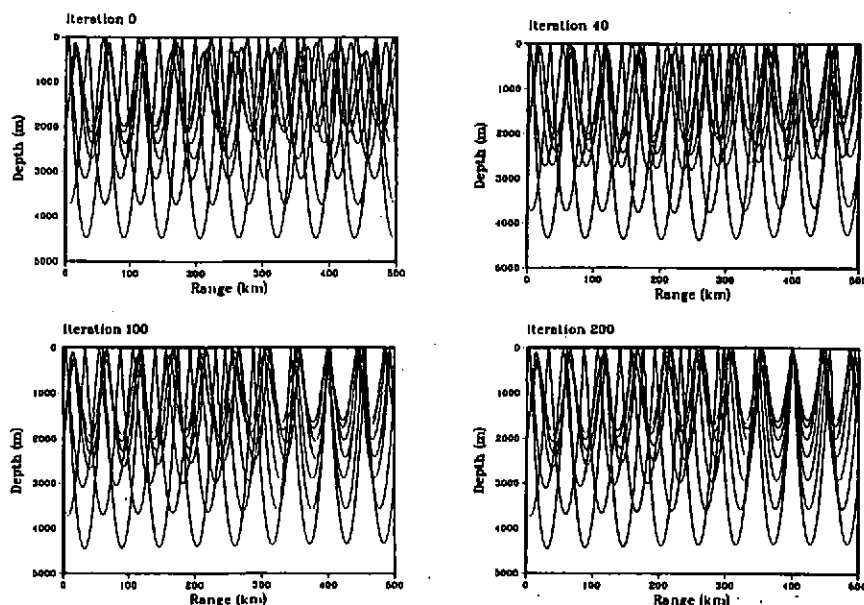


FIG 1. The back-propagated rays at various stages of the parameter search.

SOURCE LOCALIZATION

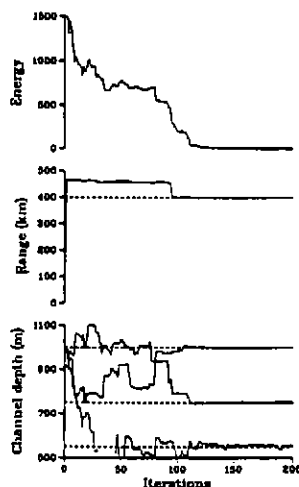


FIG 2. The energy and range and channel depth estimates for Example 1.

3. MODE-BASED FOCALIZATION

In this section, we demonstrate that it is possible to perform focalization using solutions of the wave equation. The solution of the focalization problem is often not unique because the received acoustic field is invariant under range translations of oceanographic features. When it is valid, the adiabatic normal mode model should be ideal for focalization because it does not bother to distinguish between these feature-translation ambiguities. Since focalization requires many source and receiver combinations, the precalculation implementation [8] of the adiabatic normal mode model that has been useful for MFP [9] should be very efficient.

In analogy to the ray-based focalization method, we perform focalization by back propagating the phases of the normal modes using the adiabatic normal mode approximation. The search parameters are adjusted until the adiabatic modal phases,

$$\psi_n(r) = \text{Re} \left[\int_0^r k_n(s) ds \right], \quad (3)$$

match the measured modal phases ξ_n , where k_n is the n th eigenvalue of the depth-separated wave equation. MFP is very efficient in mode space because it is possible to determine source range and source depth separately [10,11].

We apply the following high-resolution cost function E for mode-based focalization:

SOURCE LOCALIZATION

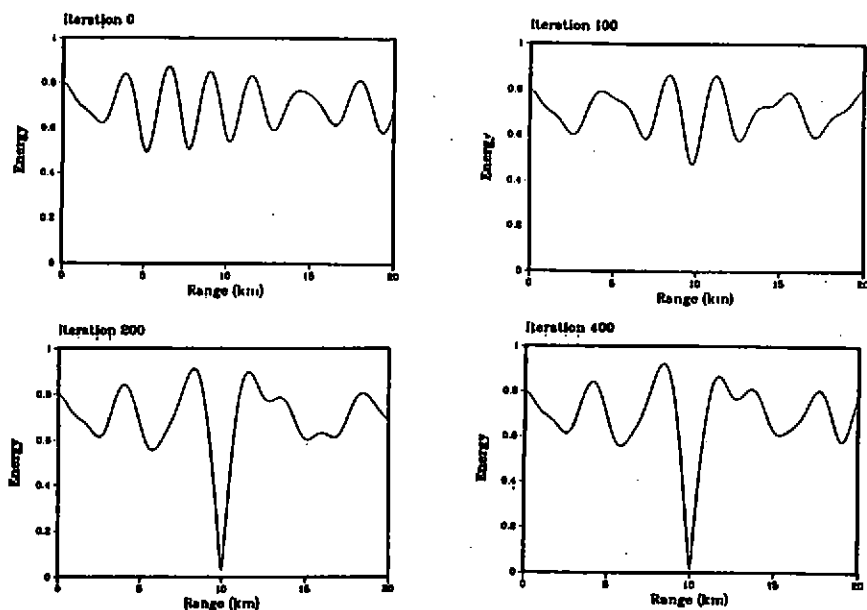


FIG 3. The modal phase function for Example 2 at various stages of the parameter search.

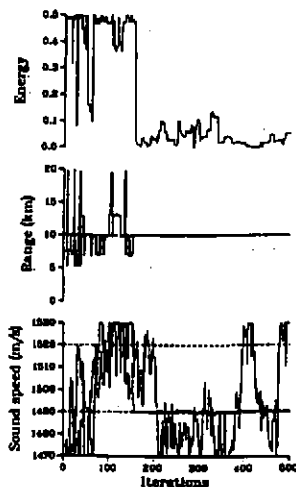


FIG 4. The energy and range and sound speed estimates for Example 2.

SOURCE LOCALIZATION

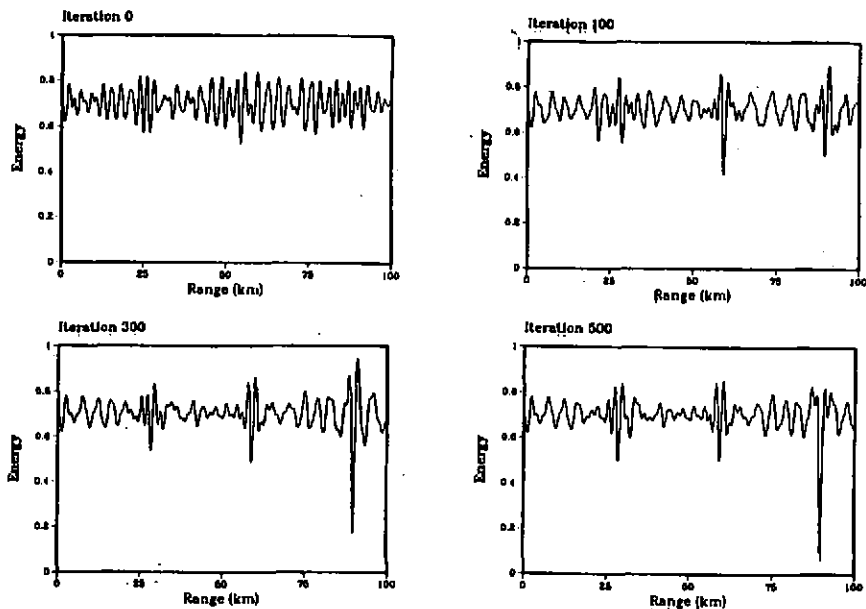


FIG 5. The modal phase function for Example 3 at various stages of the parameter search.

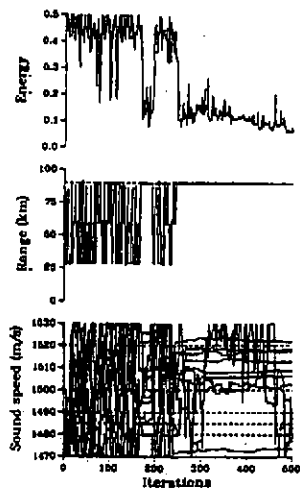


FIG 6. The energy and range and sound speed estimates for Example 3.

SOURCE LOCALIZATION

$$E = \min_r F(r), \quad (4)$$

$$F(r) = \sqrt{\frac{1}{N-1} \sum_{n=2}^N \sin^2 [\xi_n - \xi_{n-1} - \psi_n(r) + \psi_{n-1}(r)]}, \quad (5)$$

where N is the number of modes used for focalization. Since the difference between eigenvalues is relatively small, the differential modal phases appearing in Eq. (5) vary much slower than the modal phases. Thus F has a relatively wide peak at the source range. This is an attractive property because it allows a sparse sampling of F in range [3]. As with the ray-based focalization algorithm, the estimate at each iteration for the source range is the range at which the minimum of F occurs.

Each time the waveguide properties are varied, it is necessary to compute the k_n at many ranges to evaluate the cost function. It would be very inefficient to do this by repeatedly solving the eigenvalue problem. The k_n can be evaluated efficiently by parameterizing the environment and solving the eigenvalue problem for a set of representative realizations of the environment before performing focalization and interpolating the k_n during the focalization process.

To illustrate the performance of mode-based focalization, we consider two examples involving a time-harmonic source in an ocean of depth $d = 500$ m. The sound speed in the water column is

$$c(r, z) = c_0 + [c_1(r) - c_0](d - 2z) / d. \quad (6)$$

The sound speed at $z = d/2$ is $c_0 = 1500$ m/s. The sound speed at the ocean surface is $c_1(r)$, which is defined at equally-spaced range nodes with linear interpolation between nodes. The acoustic parameters are assumed to be known in the sediment. Since the sound speed is required at the array to measure the modal phases, it is assumed to be known at $r = 0$.

For Example 2, a 50-Hz source is located at $r = 10$ km, and two sound-speed nodes are spaced 10 km apart. The sound-speed parameter at $r = 20$ km does not influence the acoustic field incident on the array. We perform focalization using the first eight normal modes. The function F appears in Figure 3 at various stages of the search process. Initially and at 100 iterations, the energy oscillates about the expected value of $1/\sqrt{2}$ and does not approach zero at any range. At 200 and 400 iterations, the F curve has a small minimum at the source range. The energy, range estimates, and sound-speed parameter estimates appear in Figure 4. The source range and the sound-speed parameter at the source range lock in to the correct values after less than 100 iterations.

For Example 3, a 100-Hz source is located at $r = 90$ km, and ten sound-speed nodes are spaced 10 km apart. The node at $r = 100$ km does not affect the acoustic field incident on the array. Focalization is performed using twenty normal modes. The function F appears in Figure 5 at various stages of the search process. For the initial sound-speed guess, the energy oscillates about

SOURCE LOCALIZATION

the expected value and does not approach zero at any range. At 100 iterations, the modal phases are attempting to focus near $r = 60$ km. At 300 iterations, the modal phases begin to focus at the source range. At 500 iterations, the F curve has a small minimum at the source range. The energy, range estimates, and sound speed parameter estimates appear in Figure 6. During the first 250 iterations, the modal phases decide whether to focus at $r = 30$ km, $r = 60$ km, or $r = 90$ km. Despite the fact that the sound-speed parameters do not converge to the correct values, the source range locks in to the correct value after about 250 iterations.

4. CONCLUSION

Focalization is a generalization of MFP that has the primary goal of localizing an acoustic source in a waveguide with unknown acoustic properties. Focalization is effective at this task even if the waveguide parameters do not converge to the correct values. Since the received acoustic field is less sensitive to range translations of environmental features than to translations of source location, the solution for the environment is often not unique. If a sufficient volume of acoustic data is available, however, focalization is capable of determining waveguide properties.

5. REFERENCES

- [1] H P BUCKER, 'Use of Calculated Sound Fields and Matched-Field Detection to Locate Sound Sources in Shallow Water,' *J Acoust Soc Am*, **59** p368 (1976)
- [2] A B BAGGEROER, W A KUPERMAN & H SCHMIDT, 'Matched Field Processing: Source Localization in Correlated Noise as an Optimum Parameter Estimation Problem,' *J Acoust Soc Am*, **83** p571 (1988)
- [3] H SCHMIDT, A B BAGGEROER, W A KUPERMAN & E K SCHEER, 'Environmentally Tolerant Beamforming for High-Resolution Matched Field Processing: Deterministic Mismatch,' *J Acoust Soc Am*, **88** p1851 (1990)
- [4] N METROPOLIS, A W ROSENBLUTH, M N ROSENBLUTH, A H TELLER & E TELLER, 'Equations of State Calculations by Fast Computing Machines,' *J Chem Phys*, **21** p1087 (1953)
- [5] S KIRKPATRICK, C D GELLATT & M P VECCHI, 'Optimization by Simulated Annealing', IBM Thomas J Watson Research Center, Yorktown Heights, New York (1982)
- [6] M D COLLINS, 'A Nearfield Asymptotic Analysis for Underwater Acoustics,' *J Acoust Soc Am*, **85** p1107 (1989)
- [7] W H MUNK, 'Sound Channel in an Exponentially Stratified Ocean, with Application to SOFAR', *J Acoust Soc Am*, **55** p220 (1974)
- [8] W A KUPERMAN, M B PORTER, J S PERKINS & R B EVANS, 'Rapid Computation of Acoustic Fields in Three-Dimensional Ocean Environments,' *J Acoust Soc Am*, **89** p125 (1991)

SOURCE LOCALIZATION

- [9] J S PERKINS & W A KUPERMAN, 'Environmental Signal Processing: Three-Dimensional Matched-Field Processing with a Vertical Array,' *J Acoust Soc Am*, **87** p1553 (1990)
- [10] T C YANG, 'A Method of Range and Depth Estimation by Modal Decomposition,' *J Acoust Soc Am*, **82** p1736 (1987)
- [11] E C SHANG, 'An Efficient High-Resolution Method for Source Localization Processing in Mode Space,' *J Acoust Soc Am*, **86** p1960 (1989)